DOT/FAA/AM-04/18
Office of Aerospace Medicine
Washington, DC 20591

Evaluation of a Head Injury Criteria Component Test Device

Richard L. DeWeese
David M. Moorcroft

Civil Aerospace Medical Institute
Federal Aviation Administration
Oklahoma City, OK 73125

November 2004

Final Report

U.S. Department of Transportation
Federal Aviation Administration

NOTICE

Technical Report Documentation Page

1. Report No.	2. Government Accession No.	3. Recipient's Catalog No.
DOT/FAA/AM-18		

4. Title and Subtitle	5. Report Date
Evaluation of a Head Injury Criteria Component Test Device	November 2004
	6. Performing Organization Code

7. Author(s)	8. Performing Organization Report No.
DeWeese RL, Moorcroft DM	

9. Performing Organization Name and Address	10. Work Unit No. (TRAIS)
FAA Civil Aerospace Medical Institute P.O. Box 25082 Oklahoma City, OK 73125	11. Contract or Grant No.

12. Sponsoring Agency Name and Address	13. Type of Report and Period Covered
Office of Aerospace Medicine Federal Aviation Administration 800 Independence Ave., S.W. Washington, DC 20591	14. Sponsoring Agency Code

15. Supplemental Notes

This work was performed under task AM-B-03-PRS96.

16. Abstract

Aircraft seats that are certified to meet the requirements of 14 CFR Parts 23.562, 25.562, 27.562 and 29.562 must protect the occupant from serious head injury as defined by the Head Injury Criterion (HIC). Currently this is demonstrated during a dynamic sled test that includes a 50% male-size test dummy, the seat, and any surrounding aircraft structure that could be impacted by the occupant's head. To reduce cost and expedite design and certification, a means of demonstrating compliance using a component-level test was desired. A project to develop a component test method was initiated by the FAA Technical Center's Materials and Structures Branch, under contract to the National Institute for Aviation Research (NAIR) at Wichita State University (WSU). This effort resulted in the development of the HIC Component Test Device (HCTD) as described in FAA report DOT/FAA/AR-02-99. The HCTD consisted of a test dummy head attached to a pivoted arm that is propelled in an arc by an air actuator. The device was transferred to CAMI in Dec. 2002 for evaluation and further development.

A series of sled and component tests were conducted to evaluate the HCTD's predictability, repeatability, and degree of correlation with the sled tests. The device produced head impact velocity and HIC results that were very repeatable when impacting surfaces with consistent force/deflection properties. A relationship for impact velocity versus firing pressure was also developed. Several representative aircraft interior surfaces were tested at various head impact velocities and impact angles. These surfaces included padded rigid walls, unpadded composite walls and wall sections, and energy absorbing and non-energy absorbing seat backs. When the results for the two test methods were compared, impacts with some surfaces showed correlation and some did not. Impacts with padded rigid walls correlated well, while impacts with stiff walls or wall sections did not. Impacts with seat backs yielded mixed results with correlation being dependent on the stiffness of the area of the seat back being impacted. A MADYMO computer model was developed to investigate factors that could improve correlation. Further investigation is necessary to determine if modifications to the device could improve the degree of correlation.

17. Key Words	18. Distribution Statement
Head Injury Criterion (HIC), Component Test, MADYMO, Aircraft Seat Test, Simulation	Document is available to the public through the National Technical Information Service, Springfield, Virginia 22161

19. Security Classif. (of this report)	20. Security Classif. (of this page)	21. No. of Pages	22. Price
Unclassified	Unclassified	20	

Form DOT F 1700.7 (8-72) Reproduction of completed page authorized

ACKNOWLEDGMENTS

The authors gratefully acknowledge the efforts of the students and staff of the National Institute for Aviation Research Computational Mechanics Laboratory who assisted us with the transition of the HIC Component Test Device to CAMI. They made many trips to CAMI to assist with system setup, control software development, and computer simulations. Among those who contributed, our special thanks go to:

Dr. Hamid Lankarani
Gunesh Prasanna Kanetkar
Cheriyan Sony Koshy
Harishanker Nagarajan
Venkatramana Prabhala
Kendale Anant Sadanand
Lalitkumar Vasantkumar Sahare
Satish Chandra Swargam
Chandrashekhar Kalyandao Thorbole

Evaluation of a Head Injury Criteria Component Test Device

INTRODUCTION

Aircraft seats that are certified to meet the requirements of Title 14 of the Code of Federal Regulations (CFR) Parts 23.562, 25.562, 27.562 and 29.562 (1) must protect the occupant from serious head injury as defined by the Head Injury Criterion (HIC). Currently this is demonstrated during a dynamic sled test that includes a 50% male-size test dummy, the seat, and any surrounding aircraft structure that could be impacted by the occupant's head. A means of demonstrating compliance using a component-level test to reduce requirements for dynamic sled testing was desired. The objective of component-level testing was to reduce the cost of demonstrating compliance, provide seat manufacturers a method to expedite design and testing of HIC-related factors prior to certification, and provide data to support approval for certification. Component-level testing could also be used to develop material and structures specifications for items that affect the HIC results.

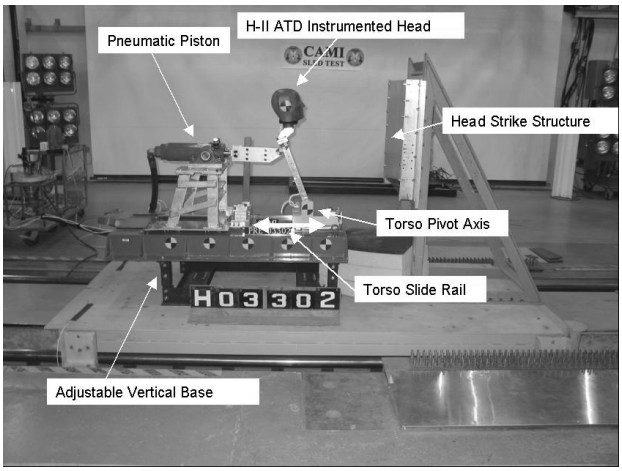

Figure 1. HCTD Description

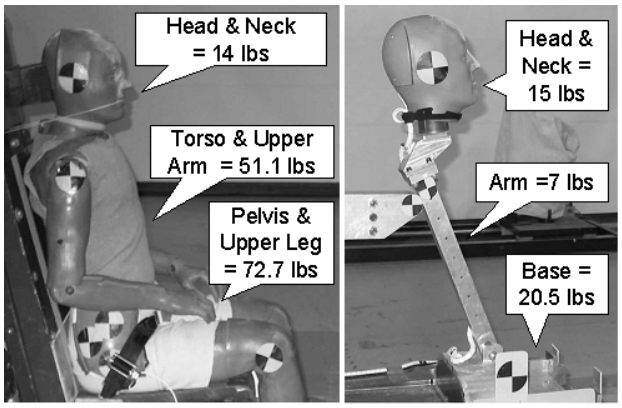

Figure 2. Mass Distribution Comparison

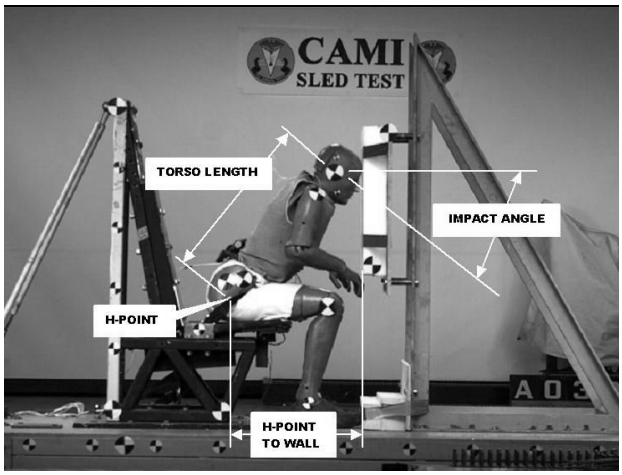

Figure 3. Sled Test Dimensional Parameters

Background

A project to develop a component test method was initiated by the Federal Aviation Administration (FAA) Technical Center, Materials and Structures Branch, under contract to the National Institute for Aviation Research (NAIR) at Wichita State University (WSU). Results of that development effort are provided in FAA Report DOT/FAA/AR-02-99 (2). To determine if the device developed by the NAIR could effectively demonstrate compliance with FAA Regulations, the device was transferred to CAMI in Dec. 2002 for evaluation and further development.

System Description

Figure 1 shows the HIC Component Test Device (HCTD) as it was configured for the evaluation tests described in this report. The impact arm consists of a Hybrid II Anthropomorphic Test Dummy (ATD) head mounted to an arm that is pivoted at the opposite end. Unlike the test dummy that has a flexible, rubber neck, the HCTD neck connecting the head to the pivoting arm is made from rigid polycarbonate. The arm pivot is mounted to a block that is free to slide aft during device actuation. As shown in Figure 2, the mass distribution of the HCTD is quite different from the Hybrid II ATD. The dimensions and kinematics of the device are meant

to replicate a 50% male-size ATD restrained by a lap belt during a forward-facing sled test. Figure 3 illustrates the pertinent dimensional parameters corresponding to the sled tests, and Figure 4 illustrates the parameters for the HCTD.

The following sequence of events occur during device operation:

1. Prior to each test, the accumulator is slowly charged to the required pressure with nitrogen.
2. When the test begins, a valve is quickly opened, allowing the nitrogen stored in the accumulator tank to flow to the air cylinder.
3. The air cylinder in turn actuates a linkage that pushes the arm forward so that the head travels in an arc.
4. When the air cylinder reaches the end of its travel, the actuation linkage stops.
5. The head continues to travel in an arc at near-constant speed until it impacts the surface being tested.

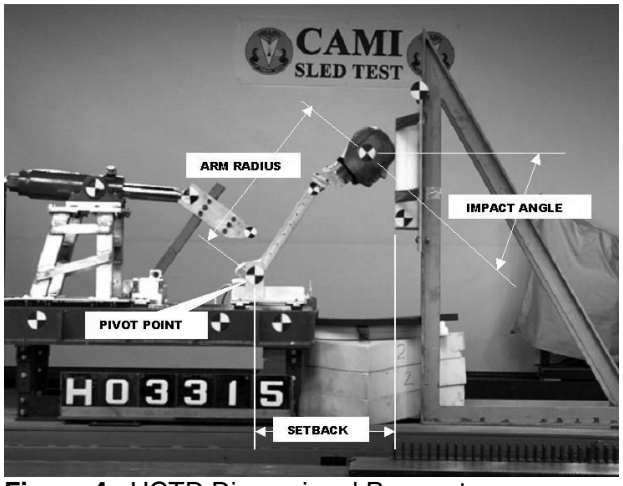

Figure 4. HCTD Dimensional Parameters

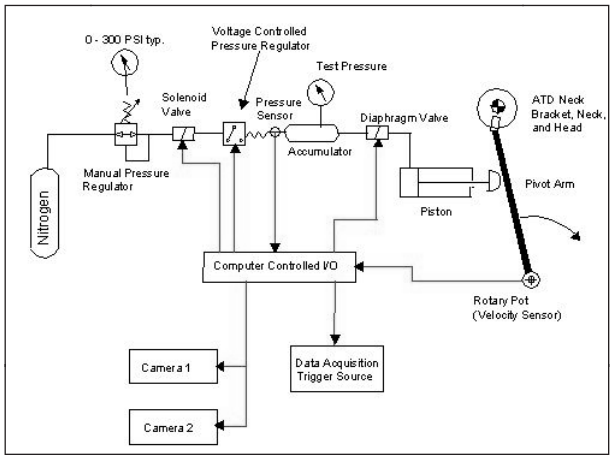

Figure 5. System Schematic

The head velocity is a function of the initial accumulator pressure. A rotational potentiometer was installed to allow real-time motion of the pivoting arm to be recorded. Since the head is rigidly fixed to the pivoting arm, head position and velocity can be derived from this recorded arm angle. However, to determine the head center of gravity (CG) position and velocity more accurately, photometric analysis was also used. Test operation is controlled by a Labview (National Instruments, Austin, Texas) program that charges the accumulator, opens the firing valve, monitors the arm rotation, and triggers the data acquisition system and high-speed cameras. A schematic of the system is shown in Figure 5.

An operational problem previously noted by NAIR was that the air cylinder was still accelerating the device arm as it contacted the test specimen, and the arm would contact the actuator linkage during rebound. Ideally, the arm should be freely coasting throughout the impact. This was corrected by moving the actuator linkage and air cylinder aft providing the necessary clearance to eliminate the problem.

Predictability and Repeatability Tests

An initial series of tests were accomplished to determine if the device could produce impact velocities that were both predictable and repeatable. A measure of repeatability for head acceleration responses was also desired.

Thin Aluminum Sheets. The first impact surface evaluated, a 2024-T3 aluminum sheet, was 28.5" W x 31" H x 0.063" T. It was bolted at the vertical edges to 4-inch-wide aluminum C-channels that were, in turn, bolted to a rigid support. This impact surface had been devised by NAIR for development purposes only and was not meant to represent any actual aircraft interior surface. When impacted in the center, the aluminum sheet bowed forward and the C-channel supports flexed inward. Our test results are compared with the NAIR results in Table 1. This table shows the accumulator pressure, head velocity, impact angle, and HIC results of two tests conducted by NAIR and three conducted by CAMI using this surface. CAMI's HIC results for this surface varied widely and differed significantly from the NAIR results. It was determined that the performance of this impact surface is very sensitive to installation details. Since the aluminum support channels were deforming plastically during each test, each new aluminum sheet installed had to be match drilled to fit to get consistent boundary conditions. Achieving a precise fit along each edge was not considered a practical solution and would still not address the progressive permanent deformation of the support channels that could also be contributing to the inconsistent performance.

Table 1. Initial Tests

Surface	Test ID	Pressure PSI	Head Vel. Ft/Sec	Impact Angle Degrees	HIC	HIC Duration Milliseconds	Avg. Accel During HIC G's
Thin Aluminum Sheets	(NAIR) 01057-24	150	40.9	37.0	763.0	21	67.0
	(NAIR) 01057-28	140	40.0	39.0	752.0	25	62.2
	H03-302	140	38.2	43.0	2652.0	16	121.0
	H03-303	140	36.5	43.0	911.0	22	69.3
	H03-304	133	35.2	43.0	2227.0	18	109.0
Polyethylene	H03-305	40	19.8	43.0	102.6	25	27.5
Foam Padding	H03-308	40	18.0	43.0	105.0	18	27.0
	H03-306	80	29.2	43.0	329.4	21	47.6
	H03-309	80	28.8	43.0	413.7	19	53.0
	H03-307	150	37.2	43.0	735.5	14	66.3
	H03-310	150	39.6	43.0	739.6	21	65.0
	H03-311	225	43.6	43.0	1133.5	24	73.8
	H03-312	225	43.6	43.0	1084.0	25	71.1

Polyethylene Foam Padding. For this initial series of tests, a simple surface that would provide consistent HIC results was needed in order to evaluate the HCTD's repeatability. A 4.5"-thick stack of 1.6 lb/cu ft density polyethylene flotation foam, covered with 0.5" of soft polyurethane foam, was chosen to meet this need. The foam stack was taped to a smooth, rigid wall, but the foam sheets comprising the stack were not bonded together or to the wall. When impacted, the foam compressed and slipped downward somewhat. The test results for this surface are also provided in Table 1. This table summarizes eight tests conducted at accumulator pressures of 40, 80, 150, and 225 PSI. The performance of this impact surface was very consistent and produced a predictable relationship between impact velocity and HIC, as shown in Figure 6. Also, the low HIC results provided by these foam pads were somewhat surprising since other resilient foams previously tested had performed poorly. (3) The pad's freedom to slide vertically during the impact appears to contribute significantly to reducing HIC values.

Repeatability Results. Some of the polyethylene foam pad tests and several of the tests accomplished later in the program were repeated at various accumulator pressures to determine if the device could produce repeatable velocities. Three tests were accomplished at approximately 150 PSI, five at 200 PSI, three at 225 PSI, and nine at 262 PSI. These repeated tests are summarized in Table 2, which provides the velocity, average velocity and velocity variation for each pressure. At 262 PSI (the pressure range used to replicate head impacts with seatbacks), the demonstrated repeatability for 50.7 ft/s velocity was ± 1.2 ft/s. The repeatability of the head acceleration response was determined from two identical tests using the polyethylene foam pad (H03-311 and H03-312). At the 43.6 ft/s impact velocity achieved for these tests, the average HIC value was 1109, and the variation was ± 25. Overall, the repeatability of the device relative to head velocity and HIC was deemed to be sufficient for the intended purpose.

Predictability Results. The results of these preliminary tests were used to derive the accumulator pressure versus head CG velocity relationship. As testing continued, it was determined that a change in the initial position of the pivot point would increase the mechanical advantage of the air cylinder, thus allowing higher velocities to be generated. Figure 7 shows the pressure vs. velocity relationship derived for both the initial and improved geometries. While a clear trend exists, the data spread tends to increase with pressure. This relationship was continually revised as more tests were accomplished, but the degree of uncertainty did not improve. Fortunately, the device's good velocity repeatability enables us to overcome the less-than-optimum predictability. In practice, "trial runs" can be done to dial in the desired velocity before placing the item to be struck in front of the device.

Impact Tests of Representative Aircraft Interior Surfaces

A series of sled tests and HCTD tests were accomplished to determine the HCTD's performance when impacting typical aircraft interior surfaces. These tests evaluated the HCTD's performance over the range of contact areas, head impact velocities, and impact angles that could be encountered during certification tests involving realistic

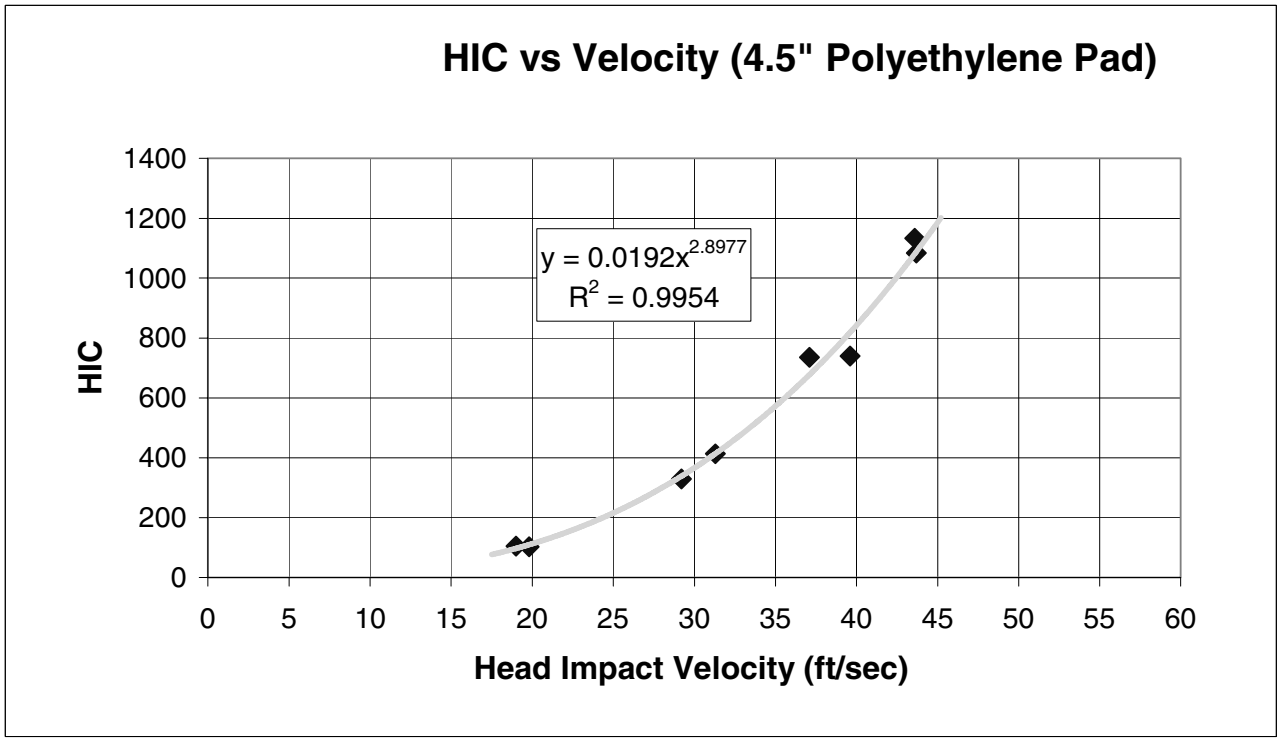

Figure 6. HIC vs. Head Impact Velocity

Table 2. Velocity Repeatability Tests

Test #	Geometry	Pressure PSI	Velocity Ft/Sec	Avg. Ft/Sec	Variation Ft/Sec
H03-307	Initial	150	37.2	37.9	1.4
H03-310	Initial	150	39.6		
H03-314	Initial	148	36.9		
H03-315	Initial	200	40.3	39.2	1.3
H03-317	Initial	200	39.5		
H03-318	Initial	200	39.0		
H03-319	Initial	200	39.3		
H03-325	Initial	200	37.7		
H03-328	Final	225	47.0	46.0	0.9
H03-329	Final	225	45.8		
H03-333	Final	225	45.2		
H04-301	Final	262	51.3	50.7	1.2
H04-302	Final	262	50.6		
H04-303	Final	262	50.8		
H04-304	Final	262	51.5		
H04-305	Final	262	51.6		
H04-306	Final	262	50.5		
H04-307	Final	262	51.0		
H04-308	Final	262	50.0		
H04-309	Final	262	49.2		

surfaces. It was expected that for these surfaces, the critical parameters of head impact velocity, impact angle, and point of contact would significantly affect the magnitude of the head accelerations measured. In dynamic impact tests, these critical parameters are dependent on the sled velocity, sled deceleration pulse, and the position of the surface with respect to the sled occupant. To allow determination of a deceleration profile and impact surface position that would produce the critical parameters desired, a MADYMO (TNO, The Netherlands) computer model was developed to predict occupant kinematics. Use of the model greatly reduced the number of trial runs that otherwise would have been necessary.

The sled tests utilized a rigid seat with a lap belt restrained Hybrid II, 50%-size ATD. The head velocity, impact angle, and point of impact on the evaluation surface were derived from the high-speed video of each sled test using the photometric analysis procedures found in SAE ARP 5725 (4). For the corresponding HCTD tests, the relative position between the HCTD and the evaluation surface, as well as the accumulator pressure, was set to reproduce these critical values as closely as practical. Table 3 summarizes the results of this test series. This table provides a comparison of the HCTD and sled tests, showing the head velocity, head impact angle, and the HIC and HIC duration for various aircraft interior surfaces described as follows:

Polyethylene Foam Pad. To represent a heavily padded interior wall, a 4"-thick block of 1.7 lb/cu ft density, polyethylene foam was taped to a smooth, rigid wall, as shown in Figure 8. During the head impact, the foam block was compressed and slid down the wall. As with the foam used in the initial tests, the impact results showed good repeatability.

Fiberglass-Faced, Aluminum Honeycomb. To represent a section of a galley wall with interior bracing, a 24' W x 24" H x 1" T piece of fiberglass-faced, 3/8"-cell aluminum honeycomb was supported along all four edges by a rigid frame, as shown in Figure 9. NAIR had evaluated 48" W x 48" H x 1" T panels of this material (referred to as Series III) in a previous study (5). The frame's interior dimensions were 20" W x 19.5" H. The panel was clamped along the top edge and supported along the bottom to prevent it from slipping. When struck, the panel dented significantly in the center. As expected, the amount of deformation increased as the head impact velocity increased.

Narrow, Fiberglass Faced, Nomex Honeycomb Panels. To represent a small closet wall, a 24" W x 48" H x 1" T piece of fiberglass-faced, 1/8"-cell Nomex honeycomb was clamped along the top and bottom edges, as shown in Figure 10. The wall face was carpeted. NAIR had evaluated 48" W x 48" H x 1" T panels of this material (referred to as Series II) in a previous study (5). When

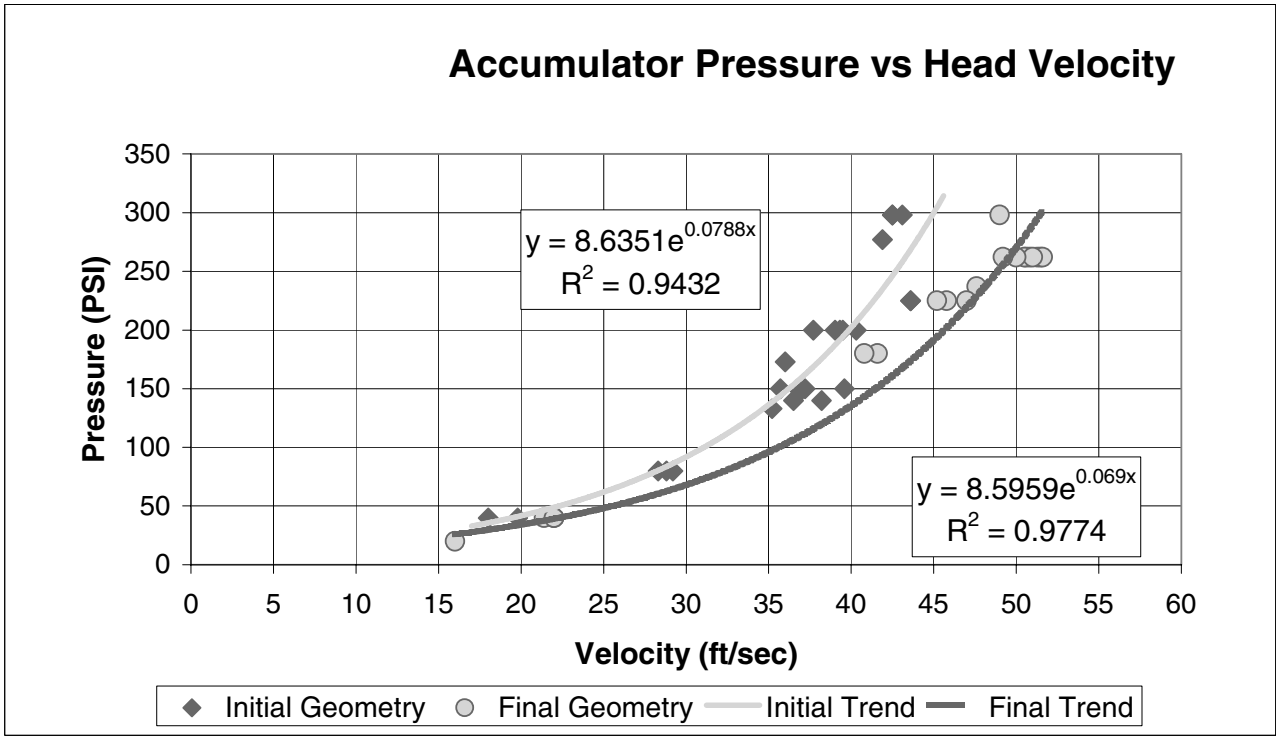

Figure 7. Pressure vs. Head Impact Velocity

Table 3. Aircraft Interior Surface Tests

Surface	Test ID	Head Vel. Ft/Sec	Impact Angle Degrees	HIC	HIC Duration Milliseconds
Polyethylene Foam Pad	A03007	32.2	45.7	304.3	28
	A03008	32.6	46.7	302.1	29
	H03316	28.3	43.0	400.8	19
	A03011	38.7	40.6	667.9	17
	A03013	38.7	40.6	699.1	21
	H03314	36.9	43.0	756.3	18
	A03009	42.4	41.6	1047.2	16
	A03010	43.8	42.9	1044.5	16
	H03315	40.3	43.0	918.9	23
	H03317	39.5	43.0	942.6	15
	H03318	39.0	43.0	873.6	17
	H03319	39.3	43.0	923.3	17
Fiberglass Faced, Aluminum Honeycomb	A03022	42.1	42.4	772.8	20
	H03322	41.9	42.4	726.7	26
	A03023	46.3	38.4	1009.8	21
	H03329	45.8	37.9	802.5	26
Narrow, Fiberglass Faced, Nomex Honeycomb Panel	A03015	38.0	44.6	1110.0	17
	A03018	37.9	44.1	944.4	16
	H03325	37.7	44.9	389.1	5
Wide, Fiberglass Faced, Nomex Honeycomb Panel	A03004	44.7	53.2	1084.3	7
	H03320	47.6	53.0	1420.6	23
Narrow-Body Class Divider Panel	A03028	41.6	43.8	458.2	34
	H03330	41.6	44.0	285.7	36
Wide-Body Class Divider Panel	A03027	40.5	45.8	1547.4	5
	A03034	41.3	49.5	1597.8	11
	H03331	40.8	44.0	670.6	9
EA Seat Back	A03030	48.6	30.6	639.3	30
	H03332	49.0	33.3	324.5	10
EA Seat Back with Video	A03032	49.2	35.2	789.4	5
	H03333	45.2	37.2	752.6	6

Note: Seld Test ID numbers start with "A" HCTD Test ID numbers start with "H"

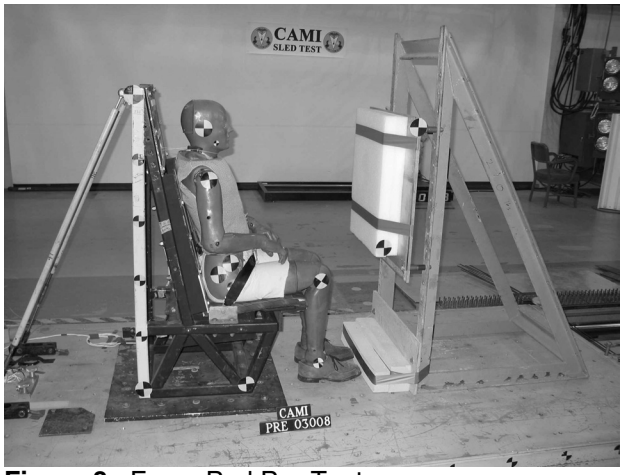

Figure 8. Foam Pad Pre-Test

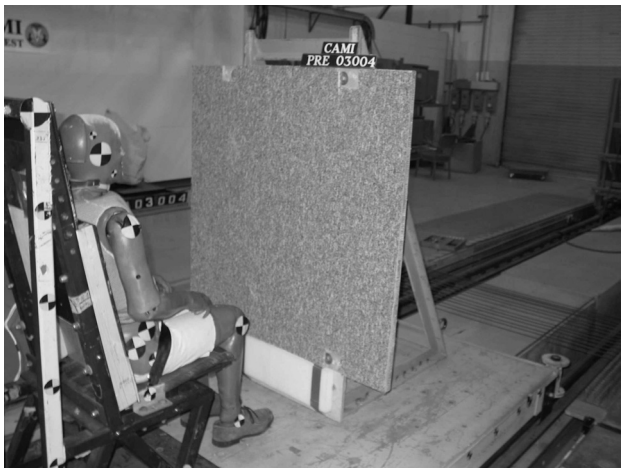

Figure 11. Wide Nomex Panel

Figure 9. Aluminum Honeycomb Post-Test

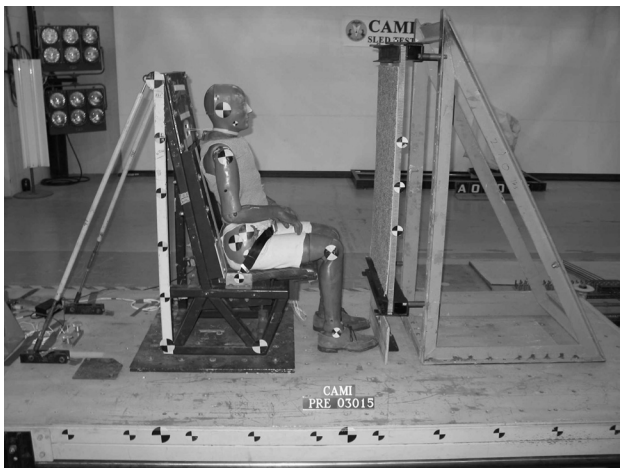

Figure 10. Narrow Nomex Panel

struck, the panel bowed in the middle, showed signs of delamination, but did not fracture.

Wide, Fiberglass-Faced, Nomex Honeycomb Panels. To investigate the affect of attachment methods, a 48" W x 48" H x 1" T piece of fiberglass-faced, 1/8"-cell Nomex honeycomb was attached to a rigid frame at four points, as shown in Figure 11. The attachments had 1.625"-thick spacers between the wall and frame, and the wall face was carpeted. At the points of attachment, the honeycomb had been filled with an epoxy potting compound to provide a solid mounting surface. The attachment points were in a rectangular pattern spaced 24" horizontally and 45" vertically. This was the same material that was used for the previously mentioned 24" W x 48" H sample tests. While this mounting method was not representative of any actual aircraft installation, it was included to determine the affect that boundary conditions have on impact performance. When struck, the wall bowed horizontally until it contacted the support frame, which was 1.625 inches away from the back surface.

Class Divider Panels. Class divider panels from narrow-body and wide-body aircraft were mounted in a fashion emulating the location and stiffness of a typical aircraft installation. The narrow-body panel was made from 1"-thick fiberglass faced, Nomex honeycomb and was attached at the top and bottom to legs that were free to pivot and lengthen as the panel bowed. Figures 12 and 13 show the mounting method in detail. The wide-body panel was much taller and was also made from 1"-thick fiberglass-faced Nomex honeycomb. It was also attached using the same method but was heavier and more rigid since the entire periphery and attachment points had been "potted" in. Figure 14 shows the panel mounted to the rigid support frame. When the narrow-body panel was struck, it bowed forward until it folded in the area near the upper attach points. When the wide-body panel was struck, the panel bowed forward until it cracked

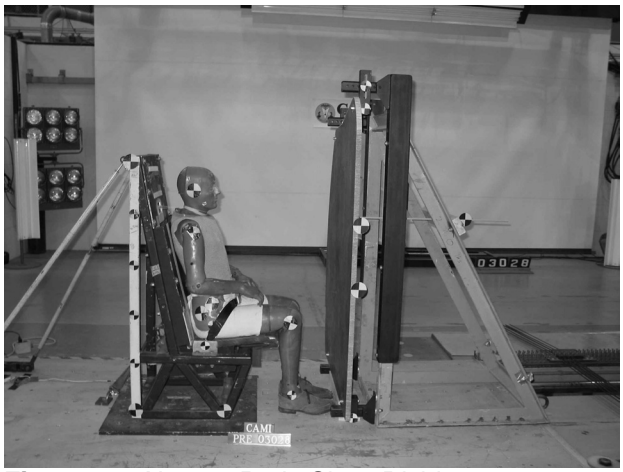

Figure 12. Narrow-Body Class Divider

Figure 13. Class Divider Mounting Detail

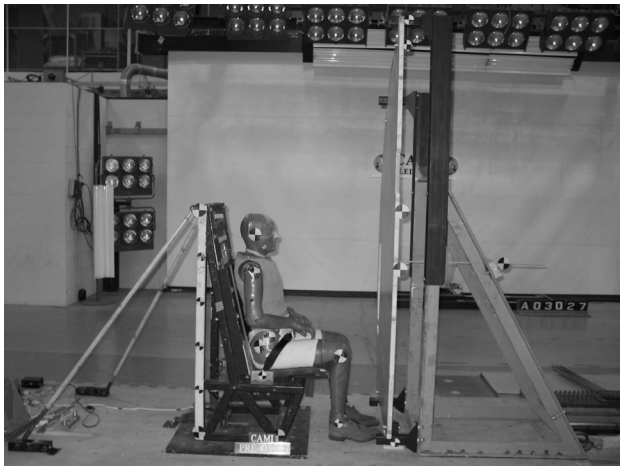

Figure 14. Wide-Body Class Divider

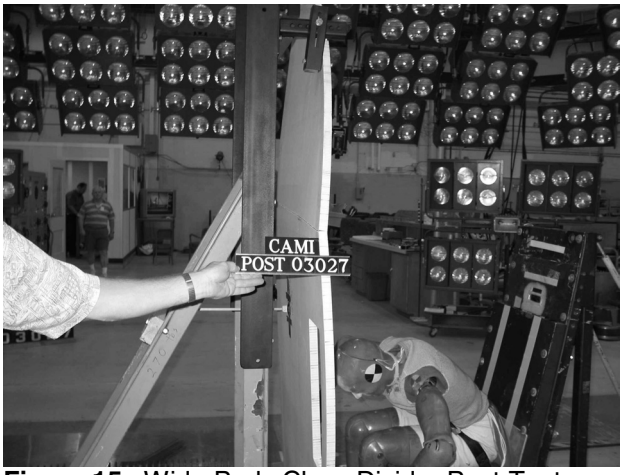

Figure 15. Wide-Body Class Divider Post-Test

horizontally at a notch 2/3 up the panel (Figure 15). A second sled test of the wide-body panel was accomplished after the horizontal crack was repaired (we only had two of these valuable samples). This test was done to verify the very high HIC measured in the first test. Both the panel response and HIC for the second test were similar to the first test.

Energy-Absorbing (EA) Seatback. A set of older, statically qualified, passenger double seats was modified by adding an energy-absorbing element to each seatback hinge mechanism. An energy absorber of this type allows the seatback to stroke forward when a force of approximately 300 lb. is applied horizontally at the top of the tray table. This stroking action can significantly reduce the probability of head injury. The area above the tray table on one set of seatbacks had a hollow cavity covered by a fiberglass shroud. The other set was modified by adding a wood block just above the tray table to emulate the weight and stiffness of a typical video screen installation (Figure 16).

During sled and HCTD tests of the hollow seatback, the head struck in the center of the seat, 3.6 inches down from the top of the seatback. The head shattered the fiberglass cover, allowing it to penetrate into the seatback cavity before pushing the entire seatback forward. During the sled and HCTD tests of the seatback that had the simulated video screen, the head struck the center of the seat, 5.4 inches down from the top of the seat. The head did not penetrate the seatback but did push the seatback forward significantly.

During the sled test, the top of the hollow seatback elastically flexed forward and then began to rebound aftward with a velocity of 8.5 ft./sec. just as the ATD stuck it. Figure 17 shows this point in time. The seatback with the video screen emulation was still flexing forward with a velocity of 3.4 ft./sec. when the ATD struck it (Figure

Figure 16. Video Screen Emulation

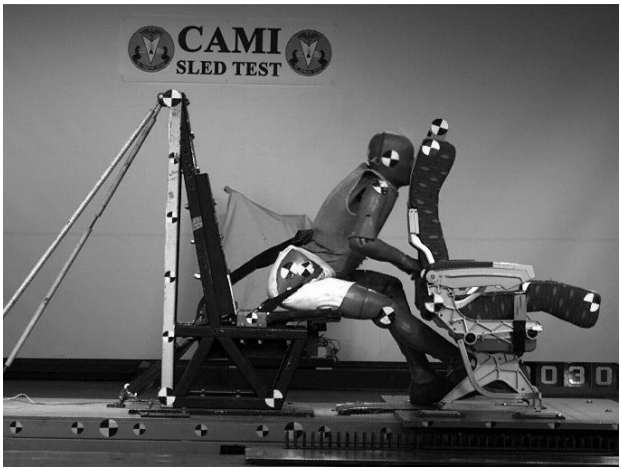

Figure 17. Hollow Seatback Impact

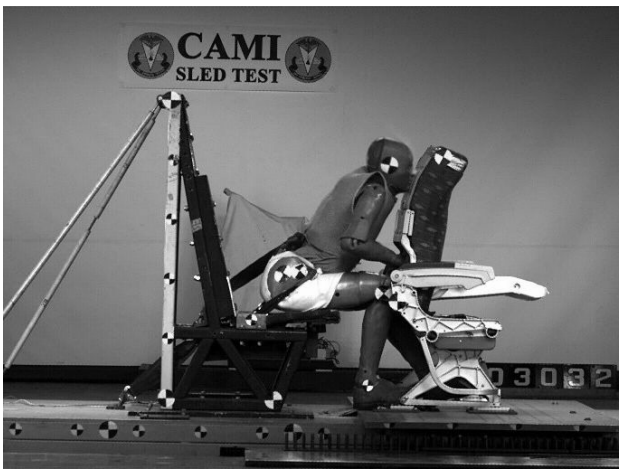

Figure 18. Video in Seatback Impact

18). To properly simulate these impacts with the HCTD, some means of compensating for the flexed location and motion of the seatbacks was needed. The seat flexure was emulated by simply pulling the backs forward with a strap to the same position as seen in the sled test. The hollow seatback was pulled forward 4.4 inches from nominal, and the seatback with the video screen emulation was pulled forward 12.1 inches. Since inducing the appropriate velocity to the seatbacks was not practical, the speed of the head impact was adjusted instead. To calculate the head velocity difference needed to compensate for seatback motion, an equivalent impact energy approach was taken. If the impact between the HCTD and the seatback is thought of as a collision between two inverted pendulums, then the combined rotational energy ($I\omega^2$) of both pendulums at the time of impact should be the same for both the sled and component test. To derive the velocity change, the mass moment of inertia (I) was measured for both the HCTD arm and each seatback, and the angular velocity (ω) was calculated for each seatback. Since the moment of inertia for the HCTD arm was much greater than the seatbacks, only a small change in velocity was necessary to compensate for the significant velocity of the seatback.

Follow-on Seatback Impact Tests

After the initial series of tests were complete (predictability, repeatability, and representative interior surfaces), the results were examined to determine the next course of action. Since the results for tourist-class passenger seatbacks showed a promising correlation trend and would be a very useful application, a follow-on series of tests was conducted to establish the level of correlation that could be achieved by the HCTD. Two locations on the seatback that are typically struck during a certification test were chosen as impact targets. The first location was at a point on the seatback centerline midway between the top of the seat and the tray table. The second location was a point offset 6" to the side at the top edge of the tray table. Figures 19 and 20 show the chalk marks left by the ATD's head at the two impact points. The seat used for the evaluation was a triple-place passenger seat with seatbacks not incorporating the dedicated energy absorption mechanisms that many recent designs do. This design, instead, relied on elastic/plastic flexing of the seatback frame to provide the necessary compliance. When a steadily increasing static load was applied horizontally at the top of the tray table, the seatback exhibited elastic behavior up to 500 lb of load and 11" of deflection, at which point the seat recline mechanism began to plastically deform until it completely failed at 13.5" of deflection. A single triple-place passenger seat

Figure 19. Center Seatback Impact Point

Figure 20. Offset Seatback Impact Point

frame was used for this entire test series. A new seatback frame, tray table, and recline mechanism were installed in the center seat position prior to each test. The area above the tray table was filled with a block of polyethylene foam encased in fire-blocking material. Since a limited number of these blocks and seat covers were available, they were reused unless obviously damaged. During the sled tests, the seatbacks exhibited the same tendency to flex forward prior to ATD impact, as seen in the previous test series. The increased stiffness of this seatback design, however, reduced the average seatback rebound velocities to 6.3 ft/s and the forward flexure to 2". The velocity of the HCTD arm was adjusted using the same equivalent energy method used in the previous seatback tests. Table 4 summarizes the results of this test series. For each group of similar tests, the table provides the head-impact velocity, impact angle, HIC, HIC duration, average HIC, and the HIC variation. In addition to the data shown in the table, the following observations were made relative to the follow-on tests:

Seatback Centered. During the three sled tests, the ATD consistently struck in the center of the seatback - 3" above the tray table - then creased the center of the tray table, shearing off the latch in the process. The seatback also showed this same damage pattern during each of the three HCTD impacts.

Seatback Offset. During the three sled tests, the ATD consistently struck 1" above the top of the tray table and 6" to the right of center, crushing the top edge of the table, then shearing the hinge on that side as the head slid down the right side of the seatback. In two of the

Table 4. Follow-on Seatback Tests

Surface	Test ID	Head Vel Ft/Sec	Impact Angle Degrees	HIC	HIC Duration Milliseconds	Avg. HIC	Variation HIC
Seatback Centered	A04075	47.4	38.5	1207.0	29	1203.9	23.0
	A04076	48.0	38.7	1179.4	25		
	A04077	47.4	38.9	1225.4	10		
	H04304	51.5	40.0	819.7	12	814.1	7.6
	H04305	51.6	40.0	804.6	12		
	H04306	50.5	40.0	818.1	12		
Seatback Offset	A04081	49.2	41.4	867.1	7	858.7	52.9
	A04082	48.1	42.9	907.3	7		
	A04083	48.8	42.8	801.6	11		
	H04307	51.0	42.6	737.9	17	764.6	103.6
	H04308	50.0	42.6	881.5	19		
	H04309	49.2	42.6	674.4	7		

Note: Seld Test ID numbers start with "A" HCTD Test ID numbers start with "H"

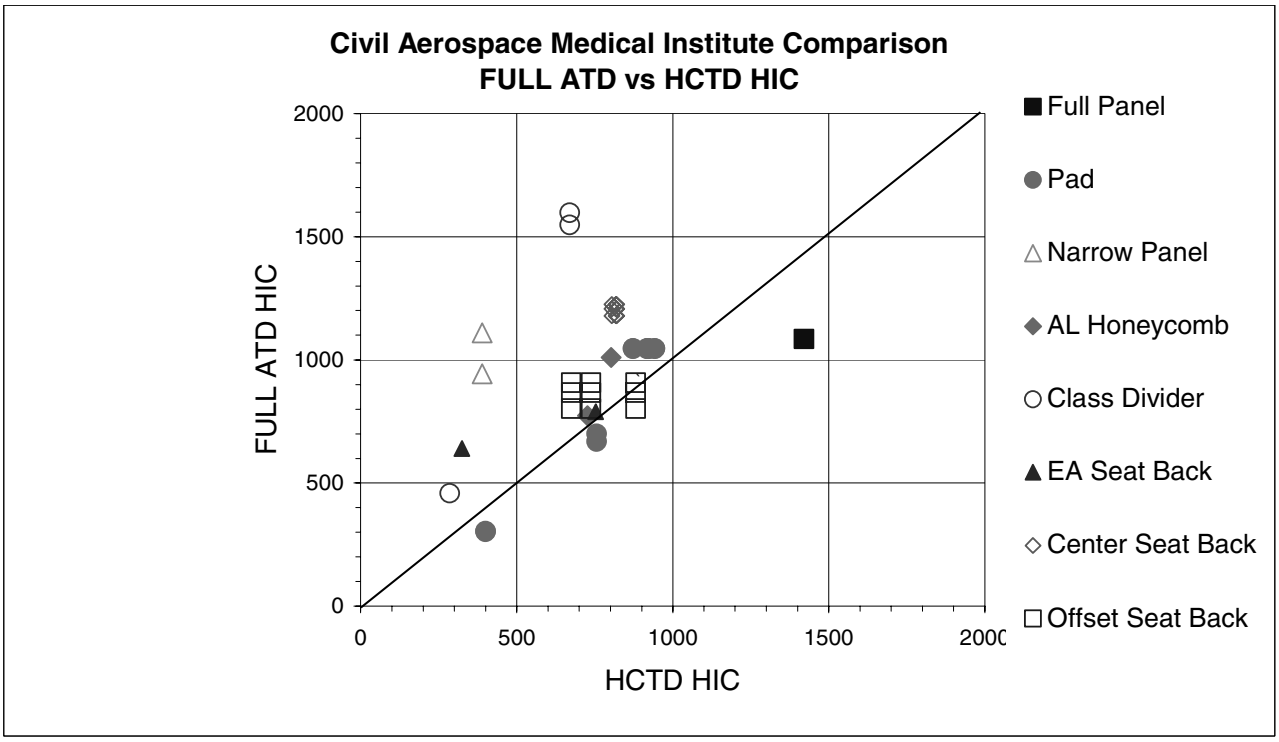

Figure 21. Full ATD HIC vs HCTD HIC

HCTD tests, the same failure mode was seen. In one of the impacts, however, the tray table hinge did not shear off. This increased the local stiffness, resulting in higher head accelerations.

Correlation Results

When the results were plotted for all of the corresponding sled and HCTD tests accomplished during CAMI's evaluation (including previous tests of various interior surfaces and the latest seatback tests), no clear correlation trend emerged (Figure 21). The degree of correlation varied significantly between the various surfaces impacted. The only discernable trend is that the correlation seemed to decrease as the stiffness of the surface being stuck increased. If correlation trends existed for clear-cut categories of surfaces such as class dividers or seatbacks, deriving a transfer function for each category could compensate for this effect. Unfortunately, as seen in the follow-on seatback impact tests, different results can be achieved when striking different parts of the same item, making this categorization difficult. NHTSA developed a component test device called the Free Motion Headform (FMH), and they were able to derive a linear transfer function and achieve an r^2 value (a standard goodness of fit measurement) of 0.97 (6). The NHTSA test data are plotted in Figure 22, which shows a clear trend between the sled and component test. One possible reason for the high degree of correlation achieved by the NHTSA may be that the surfaces the device was designed to evaluate were all very simple and similar (1" of padding on relatively stiff structure). In its current stage of development, however, the HCTD does not provide a similar level of confidence in its output when used with complex impact surfaces.

DISCUSSION

Factors Affecting Correlation. The neck flexibility and mass distribution of the HCTD is significantly different from the Hybrid II ATD used in the sled tests. This causes the head interaction with the impact surface to differ as well. In most sled tests involving impacts onto vertical surfaces, the ATD's neck flexed rearward during the period of head contact with the surface. This allowed the head to rotate rearward as it was pushed down the surface by the momentum of the ATD's torso. Since the neck of the HCTD cannot flex, and its torso is much lighter, the headform tended to not travel down the surface as far and the headform would rebound horizontally after the initial impact. Figure 23 shows the difference in head path for a typical set of corresponding tests. This difference in kinematics (after the contact with the impact surface) may be one cause for the lack of correlation between the two test methods. Since current research indicates that rapid head rotations are a potential source of brain injury (7), the inability of the device in its current form to replicate

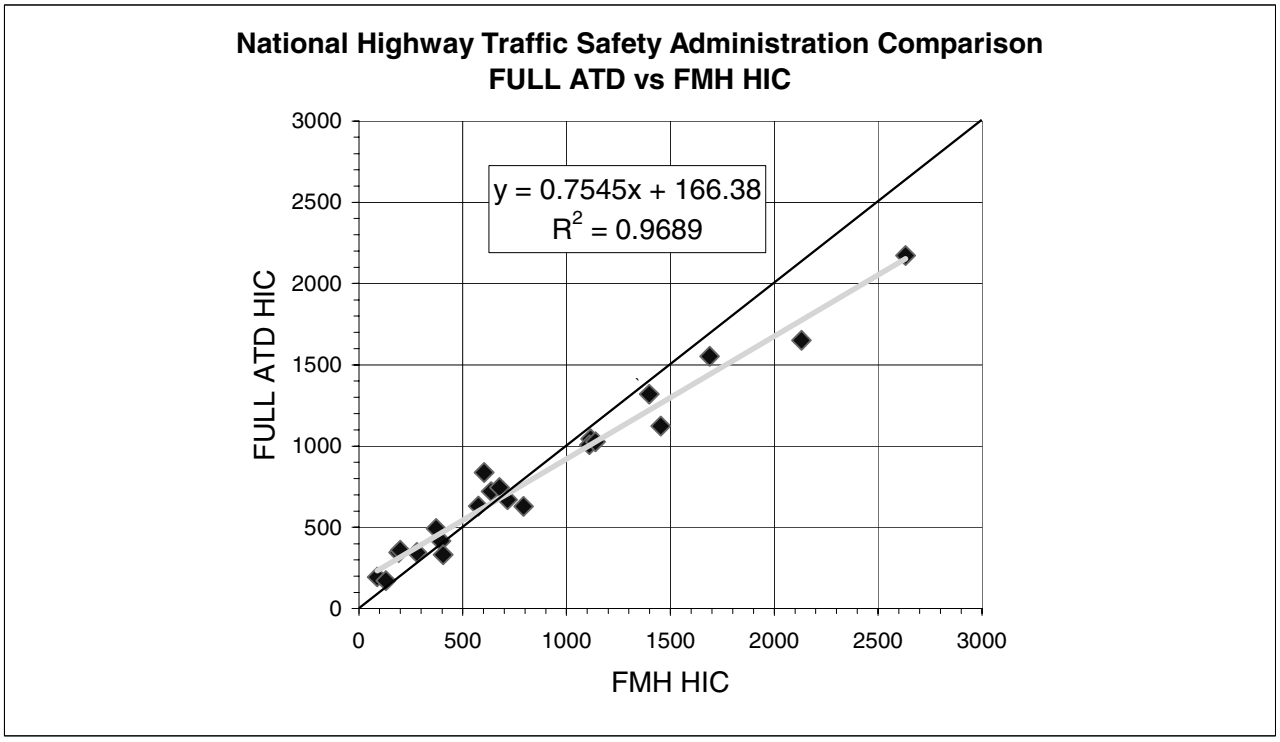

Figure 22. Full ATD HIC vs FMH HIC

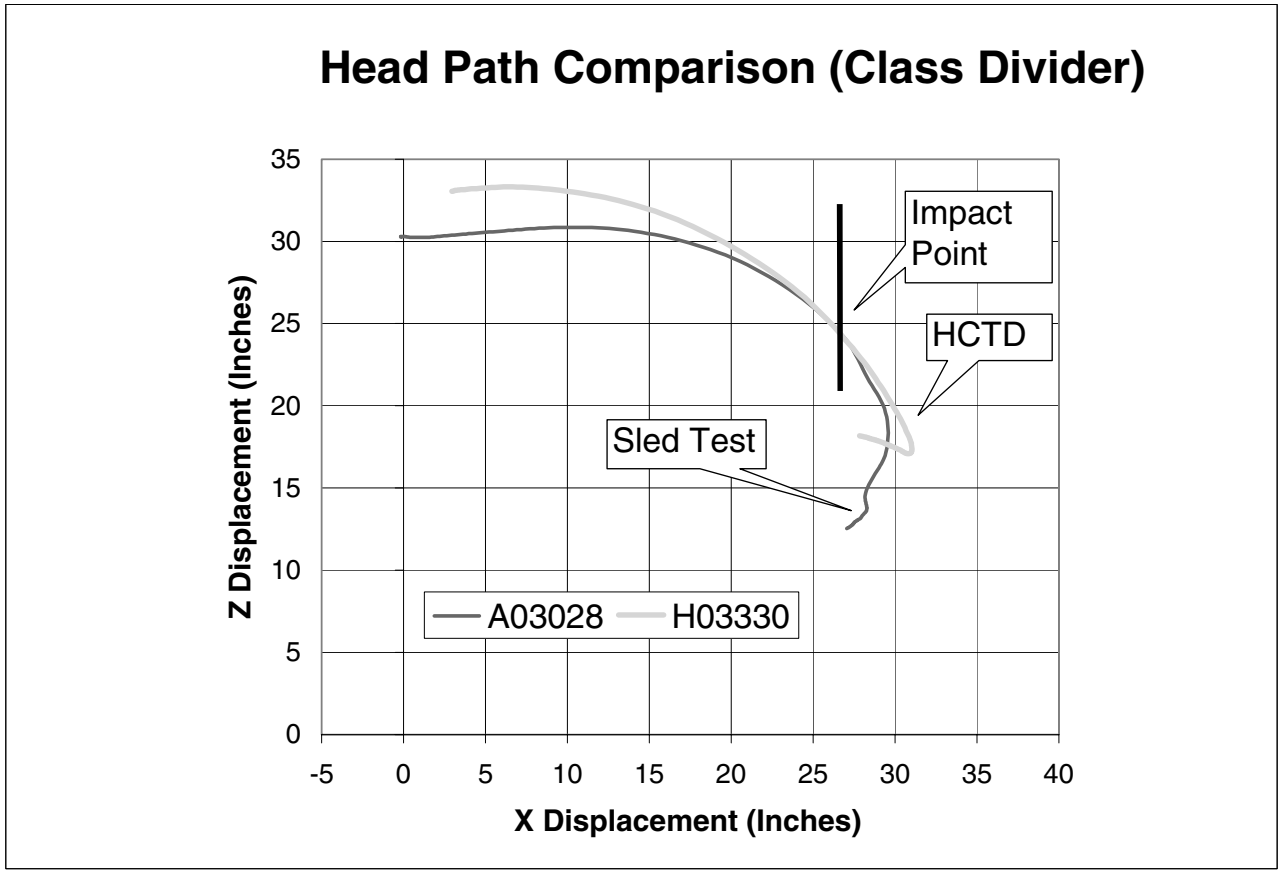

Figure 23. Head Path Comparison

Table 5. Sled Test HIC Repeatability

Surface	Test ID	Sled Vel. Ft/sec	Sled Accel G's	Head Vel. Ft/Sec	Impact Angle Degrees	HIC	HIC Duration Milliseconds	HIC Avg.	HIC Variation
Polyethylene Foam Pad	A03007	23.0	8.9	32.2	45.7	304.3	28	303.2	1.1
	A03008	23.0	8.9	32.6	46.7	302.1	29		
	A03011	29.1	10.5	38.7	40.6	667.9	17	683.5	15.6
	A03013	29.1	10.6	38.7	40.6	699.1	21		
	A03009	32.4	11.8	42.4	41.6	1047.2	16	1045.9	1.4
	A03010	34.1	11.8	43.8	42.9	1044.5	16		
Narrow, Fiberglass Faced,	A03015	29.7	10.4	38.0	44.6	1110.0	17	1027.2	82.8
Nomex Honeycomb Panel	A03018	29.1	9.7	37.9	44.1	944.4	16		
Wide-Body Class Divider	A03027	30.6	11.2	40.5	45.8	1547.4	5	1572.6	25.2
	A03034	30.6	11.5	41.3	49.5	1597.8	11		
Seatback Centered	A04075	44.6	16.3	47.4	38.5	1207.0	29	1203.9	23.0
	A04076	44.5	16.4	48.0	38.7	1179.4	25		
	A04077	44.5	16.1	47.4	38.9	1225.4	10		
Seatback Offset	A04081	44.7	16.6	49.2	41.4	867.1	7	858.7	52.9
	A04082	44.7	16.5	48.1	42.9	907.3	7		
	A04083	44.8	16.6	48.8	42.8	801.6	11		

this kinematic would limit its usefulness in measuring advanced injury assessment parameters.

The ability of the HCTD to duplicate the critical parameters of impact velocity and impact angle was limited by the practical constraints of velocity repeatability, impact angle adjustment increment, and the amount of laboratory time that could be spent repeating tests in an attempt to achieve the desired parameters. Therefore, some of the "corresponding" sled and HCTD tests shown in Table 3 had differences in these critical parameters. Since HIC is directly related to impact velocity (Figure 6), it is reasonable to assume that the differences could affect the results somewhat. If the HCTD test velocities had matched the velocity goals for all of the tests, the level of correlation might have improved for some tests, and decreased for others. Since the tests that had good velocity agreement also showed the least correlation, it is unlikely that the overall correlation for all cases would have changed significantly.

Validation Criteria Development. One of the factors needed to determine the appropriate validation criteria for a device like the HCTD is the data spread of the sled tests being emulated. If the component test device results fell within this data spread, then its accuracy in measuring HIC would be equivalent to the sled test. This high level of correlation, however, might not be necessary for a device to be useful. Since the sled tests in this study were carefully conducted so as to maximize repeatability, the results may represent the smallest data spread that could reasonably be achieved in a typical certification test. Table 5 provides a summary of the sled tests repeated during this study. As can be seen, the degree of HIC repeatability is directly related to the complexity of the item being struck. Simple items (like foam pads) had a very small amount of variation, while complex items (like seatbacks or composite wall panels) showed significant spread in the data. This could be due to slight material and manufacturing variations or small differences in the point of impact with non-homogeneous surfaces. As was observed during seatback tests, even small variations in impact point can produce a very different response. For example, in one of two otherwise identical tests, the tray table crushed, instead of shearing off. Manufacturers of aircraft interior items may want to take this natural variability into account to ensure that items falling at the extremes of the variation would still meet the required HIC limit. The small amount of variation in the foam pad tests, however, illustrates that HIC measurements from sled tests can be very repeatable.

Evaluation of Potential Modifications

A MADYMO model of the current HCTD configuration was developed to evaluate potential design changes for the HCTD. Impacts into a polyethylene foam covered rigid wall were simulated. This surface was chosen because it had been evaluated extensively during the test program and had yielded repeatable results for both the sled and component tests. The model was calibrated using

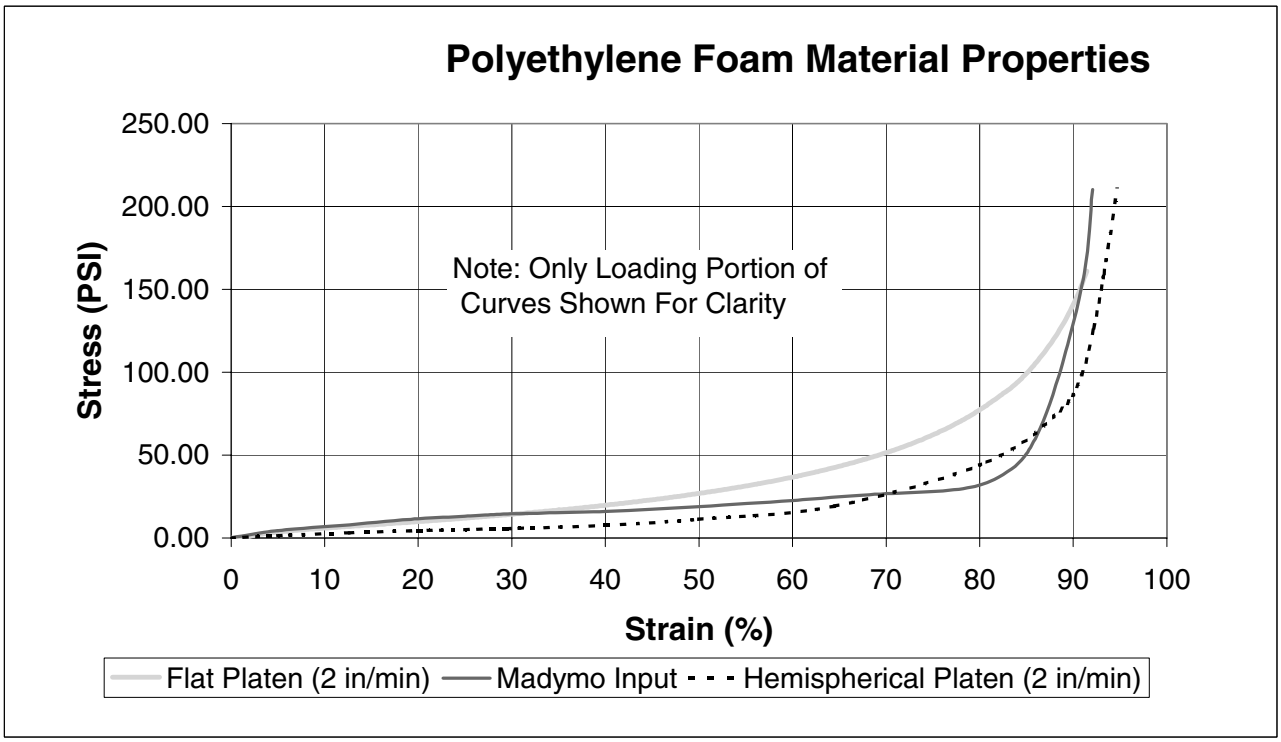

Figure 24. Foam Properties

Table 6. Simulation Results

Designator	Configuration	28.3 Ft/Sec Impact Vel.			36.9 Ft/ Sec Impact Vel.			39.5 Ft/Sec Impact Vel.		
		HIC	HIC Duration (ms)	Pad Slip (inches)	HIC	HIC Duration (ms)	Pad Slip (inches)	HIC	HIC Duration (ms)	Pad Slip (inches)
	HCTD Test (Range)	401	19.4	1.3	756	17.5	1.3	874-943	15.0-22.6	1.6-3.1
Baseline	Light - Rigid Neck	399	15.7	0.9	735	18.0	1.6	937	16.4	1.8
1	Light - Flex Neck Orientation 1	420	17.4	0.1	880	16.7	0.0	907	17.5	0.9
2	Light - Flex Neck Orinetation 2	480	16.0	0.0	762	16.4	1.2	920	16.2	1.4
3	Heavy - Rigid Neck	198	25.4	1.9	off scale	0.4	0.1	off scale	0.5	0.1
4	Heavy - Flex Neck Orientation 1	395	22.6	0.1	810	19.0	1.3	1063	20.9	0.9
5	Heavy - Flex Neck Orientation 2	500	18.9	0.0	812	18.7	1.2	981	18.7	1.6
	Sled Test (Range)	302-304	27.9-28.7	1.9-2.1	668-699	17.1-20.7	1.3-1.8	1046-1047	15.9-16.0	1.0-1.3

Modeled Test Condtion	Corresponding HCTD Test	Corresponding Sled Test
28.3 Ft/Sec, 43 degree angle	H03316	A03007 & A 03008
36.9 Ft/Sec, 43 degree angle	H03314	A03011 & A 03013
39.5 Ft/Sec, 43 degree angle	H03315 & H03317-19	A03009 & A 03010

Model Parametric	Description
Rigid Neck	Rigid Polycarbonate neck
FlexNeck	Standard test dummy rubber neck
Light configuration	42.5 lb. total system weight
Heavy configuration	138.8 lb. total system weight
Orientation 1	HCTD Head Orientation: -50 degrees from horizontal
Orientation 2	Dummy Head Orientation: -30 degrees from horizontal

an intermediate speed test, then validated using higher and lower speed tests. The model was used to evaluate the effect of neck stiffness and system mass.

Model Description. The HCTD model consists of a Hybrid II 50th percentile ATD head-neck complex attached to a rigid arm that is, in turn, pivoted from a translating rigid base. The head-neck complex is locked to the pendulum arm through a joint at the neck bracket. The head-neck complex also contains two joints to allow neck flexion. For the baseline model, both neck joints are locked at their nominal positions. A revolute joint is defined between the base and the pendulum arm to allow rotation in the x-z plane (a vertical plane aligned in the longitudinal direction). A translational joint is defined at the base to allow motion in the aft x-direction (longitudinal direction). The resultant length between the head CG and the pivot is 27.6". For the baseline configuration, the base weighs 20.5 lb, the arm weighs 7.0 lb., and the head-neck complex weighs 15 lb.

The impact surface for this series of simulations is a polyethylene foam covered wall. The wall is modeled as a rigid plane. The foam was modeled as a finite element solid, 12.5" W x 18" H x 4" T. The density of the foam is 1.5 lb/ft^3, which results in a weight of 0.78 lb. The front face of the foam is 23.35" in front of the arm pivot point. At this setback distance, the head impact angle is 43°. The stress/strain properties chosen for the foam are shown in Figure 24. The coefficient of friction between the head and the foam was 0.50. The coefficient of friction between the foam and the wall was 0.54. To simulate the transition between static and sliding coefficients of friction, the foam was held in place by a free joint set to unlock when 495 lb. of vertical force is applied to the foam block.

Calibration and Validation. During all of the tests with foam-covered walls, the head compressed the foam and then forced the entire pad to slip down the wall somewhat. Therefore, to accurately model the interaction between the head and the wall, it was important to not only match the head acceleration but also the device and impact surface kinematics. The model was calibrated by adjusting the input parameters (within normal ranges) such that the head acceleration, foam z motion, foam x deformation, and HCTD base x motion replicated test H03314. Since the dynamic force-deflection properties of the foam were unknown, its properties were essentially derived during the calibration process. As seen in Figure 24, the derived dynamic response is softer than the static response measured with a flat platen but generally stiffer than the response derived from static tests with a hemispherical platen. Use of this unique stress/strain response was necessary to compensate for rate effects and the finite element model's limitations in reproducing the constitutive properties of foam material. The model was validated by comparing results from higher and lower impact velocity simulations with the corresponding tests (H03315 and H03316).

Model Use. The two main factors evaluated to determine the potential for better correlation between the HCTD and a full sled test were neck flexion and system weight. Each was evaluated separately and then combined to produce six model configurations. To model a flexible neck, the head-neck complex from the MADYMO Hybrid II dummy was unlocked. The neck consists of two joints, with joint resistance properties unchanged from the complete dummy. The flexible neck model was simulated in two configurations, first with the neck in the un-flexed state such that at impact, the head orientation matched that of the component test with a rigid neck, and second in a pre-flexed configuration such that the head orientation matched that of the sled test. To evaluate the affect of system mass, the mass of the pendulum arm and base was increased to match the effective weight of the torso and pelvis of the ATD. The pendulum arm weight was increased from 7 lb. to 51.1 lb. The center of gravity of the arm was also moved from 10.6" to 15.3" above the pivot. The base weight was increased from 20.5 lb to 72.7 lb. Each factor was simulated for the three impact velocities mentioned earlier.

Computer Simulation Results. The results of the parametric study are presented in Table 6. None of the configurations showed an improvement over the baseline for all three velocities. Conversely, only configuration 3 (heavy with a rigid neck) had a definite negative effect on correlation for any of the three velocities. Further examination of the data reveals a clear relationship between the vertical pad excursion (pad slip) and HIC. Regardless of configuration, when the pad slipped less than the baseline, the HIC went up and vice versa. For this impact surface, vertical sliding is an important part of its overall force/deflection response to impact. The modifications that increased the normal force and/or reduced the vertical force on the pad (thus reducing pad vertical excursion) tended to result in higher HIC values. While this modeling exercise did not favor a particular configuration, it did reveal the complex nature of the interaction between the HCTD and the impact surface. If models are developed for the surfaces that did not correlate as well as the foam pads, then any improvement trends should become clearer.

CONCLUSIONS

At its current stage of development, the HCTD does not produce results that correlate with similar full-scale sled tests in all cases. Further investigation is necessary to determine if modifications to the HCTD can improve its degree of correlation with sled tests of actual aircraft components. While a single test device that can successfully emulate impacts with the wide variety of surfaces found in commercial transport aircraft would be advantageous, narrowing the focus of the device's usage may be necessary to achieve a useful level of correlation. If modifications are done, then the modified configuration will need to be extensively tested to validate its performance.

REFERENCES

1. Code of Federal Regulations, Title 14, Parts 23.562, 25.562, 27.562 and 29.562. Washington DC: US Government Printing Office.
2. Lankarani H. Development of a Component Head Injury Criteria (HIC) Tester for Aircraft Seat Certification. Washington, DC: Department of Transportation/Federal Aviation Administration; 2002, Nov. FAA report no. DOT/FAA/AR-02-99.
3. Gowdy V. Evaluation of the Instrumented Ball Impact Procedure to Assess Head Impact Protection in Airplanes; 1995, May. SAE Report 951166.
4. SAE International. Photometric Data Acquisition Procedures for Impact Test: 2003, Jun. Aerospace Recommended Practice 5725
5. Lankarani H. Design and Fabrication of a Head-Injury-Criteria Compliant Bulkhead. Washington, DC: Department of Transportation/Federal Aviation Administration; 2002, Dec. FAA report no. DOT/FAA/AR-02-98.
6. Willke D. Upper Interior Head Protection, Volume II: Fleet Characterization and Countermeasure Evaluation. Washington, DC: Department of Transportation/National Highway Traffic Safety Administration; 1991, Nov. NHTSA report DOT HS 807 866.
7. Takhonts EG, Eppinger RH, et. al., On the Development of the SIMon Finite Element Head Model, Stapp Car Crash Journal; 2003, Oct. 47: 107-133.